First International Symposium on Marine Propulsors
smp'09, Trondheim, Norway, June 2009

Simulating Biomimetic (flapping foil) Flows for Comprehension, Reverse Engineering and Design

Gerasimos K. Politis[1], Vassileios Tsarsitalidis[2]

[1]Associate Professor, Dep. of Naval Architecture and Marine Engineering, National Technical University of Athens, GREECE.
[2]Naval Architect and Marine Engineer, Doctoral Candidate, National Technical University of Athens, GREECE.
e-mail: polit@central.ntua.gr, billtsars@gmail.com

ABSTRACT

The problem of flow around one or more rigid or flexible wings performing unsteady motions (heaving and pitching or flapping and twisting) while travelling with a given velocity in an infinitely extended fluid, is formulated and solved using a potential based 3D BEM. Dynamic evolution of unsteady trailing vortex sheets is calculated by applying the kinematic and dynamic boundary conditions as part of a time stepping algorithm used for the solution of the unsteady problem. A pressure type nonlinear Kutta condition is applied at wing trailing edges. With the proper filtering of induced velocities beautiful roll-up patterns emerge, indicating the main vortex structures by which the flapping foils develop forces. The above method has been systematically applied for one and two foil arrangements, using either rectangular or fish-tail like foils, in order to provide the propulsion designer with useful data. Comparison with experimental results shows that the method can give successful predictions at transient angles of attack as high as 35 degrees, making thus the method a useful design tool for such propulsion systems. Some results for flexible wings are also presented.

Keywords: Flapping foil propulsion; Boundary element method; Incompressible non-viscous unsteady lifting flows; Unsteady wake rollup.

1 INTRODUCTION

The history of modern research on flapping foil propulsion starts in 1936 with Gray's paradox, by which estimations of dolphin resistance based on drag coefficient, results in required power about seven times the estimated muscular power of the dolphin. Modern theoretical developments start with the works of Sir James Lighthill (1969) and T.Y. Wu. (1971). A thorough review of those theories can be found in Sparenberg (2002). With the evolution of Computers direct simulations of the fully 3D fish propulsion problems start to emerge either using 3D BEM formulations or Navier Stokes solvers. Liu and Bose (1997) presented a 3D BEM method in the lines of the commercial code VSAERO but properly adapted to treat unsteadiness of the flow. They have applied the code to study the effect of wing flexibility in the efficiency of a whale's fin. Their model uses a frozen wake assumption and a linear Kutta condition at trailing edge. Liu and Bose (1999) enrich their 3D panel code with a 2D boundary layer inner solution and apply their method to estimate the effect of shape of wing plan-form to the propulsive performance. He et al (2007) presented a 3D panel code to treat tandem oscillating foils. Zhu et al (2002) has employed a 3D panel code together with experimental data to establish the 3-d features of the flow around fish-like bodies. Borazjani and Sotiropoulos (2008) present calculation of swimming forces and efficiency of a carangiform swimmer using an unsteady 3D Navier Stokes equation solver. They find that swimming power is decreased with increasing Reynolds. They also present interesting visualizations regarding the 3D wake pattern/ vortical structure produced by carangiform swimmers. In parallel to the theoretical/numerical developments a serious effort has been given by various researchers in the experimental investigation of the fish propulsion. A detailed presentation of experimental state of the art can be found in Triantafyllou (2004). Extensive experimental work, on either single or double foil configurations, has been made by Professor Triantafyllou and its co-workers (1991, 1993, 1998, 1999, 2000, 2002, 2004).

The aim of the current work, is to provide the profession with a data base which, in addition to the existing experimental and analytical data, can be used for a preliminary selection/ optimization and design of a flapping foil propulsion system. The steps towards design of a flapping foil system are very similar to that used for designing a propeller, with the charts showing the mean thrust coefficient C_T and the (mean) efficiency $effy$ of the flapping foil system as a function of the St (Strouhal number) and the maximum angle of attack $a_{\max}$ (with respect to the phenomenal flow – e.g. Triantafyllou 2003), to take the place of the open water propeller performance diagrams. The design steps for a flapping foil system can be found in Czarnowski (1997) and Bose (2008). As with open water propeller performance charts, each $CT(St, a\max)$, $effy(St, a\max)$ diagram depends on the foil geometry i.e. foil section and plan-form and foil configuration i.e. single foil or multi-foil system.

In order to provide the propulsion designer with useful data, systematic calculations have been performed for: (a) a rectangular wing with AR=3,6 (b) a double wing with AR=2 and (c) a fish-tail like wing with AR=7.76 (tapper ratio=0.4) and two skew-back angles of 25 and 45 deg. The results are presented in the form of diagrams showing level curves of mean thrust coefficient and efficiency as functions of $St, a\max$. A number of 3D visualizations are given showing the structure of the vortical wake of the flapping foils in various loading regimes. Some comparisons with experimental results are also presented. We also give calculations of the time history of unsteady forces for a rigid and a flexible wing to be used in the future for comparison purposes with other researchers.

2 THE BEM METHOD

During the period 2002-2008 a 3D-BEM computer code has been developed by the first of the Authors, for the simulation of 3D unsteady incompressible non-viscous flow around system of bodies. Detailed Description of an initial version of the code can be found in Politis (2004, 2005). We shall now give a brief presentation of the main aspects of the code: The bodies can be rigid or flexible and can move (or deform) independently in a prescribed (determined by the user) manner. Two types of bodies are allowed: (a) non-lifting bodies and (b) lifting bodies. For the latter case the user has to determine the line of flow separation in the surface of each lifting body. The code can accept as input virtual open boundaries. With this feature, by using more than one open lifting body to describe a closed real lifting body, separation lines other than wing trailing edges can be introduced. Similarly many open non-lifting bodies can be used to simulate more complex closed non-lifting bodies such as the propeller hub and part of propeller axis. Then, during execution, a free shear layer is automatically generated by the code, from each (given) separation line, and its time evolution is determined by applying the Helmholtz vortex theorems. Shed vorticity intensity from each separation line is calculated by applying a Kutta condition. Three types of Kutta conditions can be alternatively applied by the user for the determination of the shed vorticity from lifting bodies: (a) A linear Morino condition, (b) a pressure type (nonlinear) condition and (c) a mixed (nonlinear) condition (Morino at tips – pressure type in the remaining part of the separation line). This last condition, which, as far as the authors know, is new in the field, has been dictated by the fact that at higher loadings a pressure type kutta at tips is too strong and eventually leads to a destruction of the free vortex sheet geometry at tips. The core of the code is a potential based BEM formulation of the corresponding free BVP and a time stepping algorithm. For each time step 4-node quadrilateral elements are used for the subdivision/ descritization of body and shear layer boundaries. The unknowns at each time step are the constant potential values at body elements and the constant dipole intensities on kutta strips (i.e. strips of elements directly adjacent to each separation line – Politis 2004). The resulting system of equations has a linear part related to the satisfaction of the no-entrance condition and a nonlinear part related to alternatives (b) or (c) of the kutta condition. The non-linear system is solved at each time step using Newton iteration with starting value taken from a Morino type linear kutta (first alternative). Usually three iterations are enough to converge. Calculation of free vorticity layer at each time step is accomplished using (Politis 2004):

$$\frac{D\mu}{Dt} = \frac{\partial \mu}{\partial t} + \left(> \vec{v} < \cdot \nabla\right)\mu \tag{1}$$

where the mean velocity $> \vec{v} <$ at points of the sheet is calculated using a mollifier based filtering technique to cancel out the Kelvin-Helmholz instability inherently present in such type of problems. With a careful selection of filters the main vortical structure of the shear layers, in the scale of thrust and lift producing vortices, can be emerged.

As already said the bodies comprising our system can be flexible. In this case it is impossible to define a translational or rotational velocity for each body of our system and subsequently apply the usual formulas to find the useful power of the system, termed EHP (effective horse power), or the consumed power, termed DHP (delivered horse power). For the calculation of EHP and DHP on a flexible body we use the following procedure:

Let A a point belonging to the surface S of a body of our system. Let $\vec{F}$ denote the total force exerted by the fluid to the body at A. This force is a sum of pressure forces normal to body denoted by $\vec{P}$ and viscous forces tangential to body denoted by $\vec{D}$. Thus:

$$\vec{F} = \vec{P} + \vec{D} \tag{2}$$

Viscous forces are entered in our code in the form of simple surface drag coefficient which is a function of a body Reynolds number.

Let also $\vec{v}$ denote the velocity of A with respect to an inertia reference frame. Consider also a parallel vector field $\vec{d}$ with $\vec{d}$ a unit vector. Then:

$$\vec{v} = (\vec{d}\cdot\vec{v})\cdot\vec{d} + (\vec{d}\times\vec{v})\times\vec{d} \tag{3}$$

The power done from the fluid to the body at A is given by:

$$pow = \vec{F}\cdot\vec{v} = (\vec{F}\cdot\vec{d})(\vec{d}\cdot\vec{v}) + \vec{F}\cdot((\vec{d}\times\vec{v})\times\vec{d}) \tag{4}$$

and the net power from a body or system of (flexible) bodies is given by:

$$net\_pow = \int_S \vec{F}\cdot\vec{v}\cdot dS = \int_S (\vec{F}\cdot\vec{d})(\vec{d}\cdot\vec{v})\cdot dS + \int_S \vec{F}\cdot((\vec{d}\times\vec{v})\times\vec{d})\cdot dS \tag{5}$$

In propulsion problems there is always a preferable instantaneous direction in which the system plans to move. Take $\vec{d}$ along this direction. Then the first term in the rhs of equation (5) is the instantaneous EHP and the second term is the instantaneous DHP. The ratio EHP/DHP defines the instantaneous efficiency. In our code we have create a “type coordinate system” object which is defined

by the user and which provides the necessary instantaneous vector $\vec{d}$ needed for the calculation of EHP and DHP. Finally notice that in flapping foil problems there are instances where the foil operates as a windmill, i.e. the system takes power from the flow. At those points DHP becomes eventually small (smaller than EHP) giving thus rise to instantaneous efficiencies greater than one. Notice that in case of rigid bodies the previous procedure degenerates to the usual one based on forces, moments and the instantaneous parallel translation and rotation of each rigid body.

3 GEOMETRY AND MOTION

By AR we denote the aspect ratio of the wing defined by:

$$AR = s^2 / E \tag{6}$$

where s the wing span and E the planform area of the wing. Strouhal number of the motion is defined by:

$$St \overset{def}{=} \frac{2y_0\omega}{2\pi u} \tag{7}$$

where the wing motion is defined by a parallel (along X-axis) movement with velocity u, a heave motion (along Y-axis) with amplitude y_0, a pitching motion with amplitude θ_0, a phase angle ψ, $\omega = 2\pi n$ the angular velocity of unsteady motion and n the corresponding frequency. Then the instantaneous angle of attack with respect to the phenomenal velocity is given by:

$$a(t) = \theta_0 \sin(\omega t + \psi) - \tan^{-1}\left(\frac{y_0\omega\cos(\omega t)}{u}\right) \tag{8}$$

which using the definition of the St number becomes:

$$a(t) = \theta_0 \sin(\omega t + \psi) - \tan^{-1}(\pi \cdot St \cdot \cos(\omega t)) \tag{9}$$

For each selection of the set of variables: $u, \theta_0, \psi, St, \omega$ an $a(t)$ function is uniquely defined with a maximum value (t varying) denoted by $a_{\max}$. The inverse problem i.e. given $u, \psi, St, \omega, a_{\max}$ find θ_0 cannot always have solution and if it has there would be more than one. This inverse problem can be solved by the following process. For each value of θ_0 in a given range, vary ωt (0 to 2π) and find $a_{\max}$ (one or more values). Repeat the procedure with different θ_0 until $a_{\max}$ reach the given value. Notice that in case of two solutions, only one is thrust producing i.e. relevant to our problem. This procedure has repeatedly been applied in the sequel, in order to find the necessary data for the preparation of design charts for the thrust coefficient and efficiency in various flapping foil configurations.

4 DESIGN CHARTS

4.1 Rectangular wing, AR=6.

A rectangular wing with c=0.1 m and AR= 6 has been used in this calculation, fig.1. Motion is determined by the heave amplitude $y_0 = 0.075m$ and the frequency $n = 3Hz$. Calculations of thrust coefficient C_T:

$$C_T = \frac{T}{0.5 \cdot \rho \cdot E \cdot u^2} \tag{10}$$

and efficiency (=EHP/DHP) have been made for a range of St and $a_{\max}$ (denoted by A) as shown in the figures 2 and 3 (ρ is the fluid density). For each St the corresponding advance velocity can be found from (7). Similarly for each $a_{\max}$ a θ_0 has been calculated by the procedure described previously. Finally a phase angle $\psi = 90^0$ and a NACA 0012 section has been assumed in all calculations. Calculations have been performed with a step in St of 0.05 while steps in $a_{\max}$ are 5 deg.

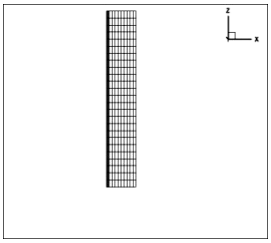

Fig. 1. Plan form of rectangular wing, AR=6

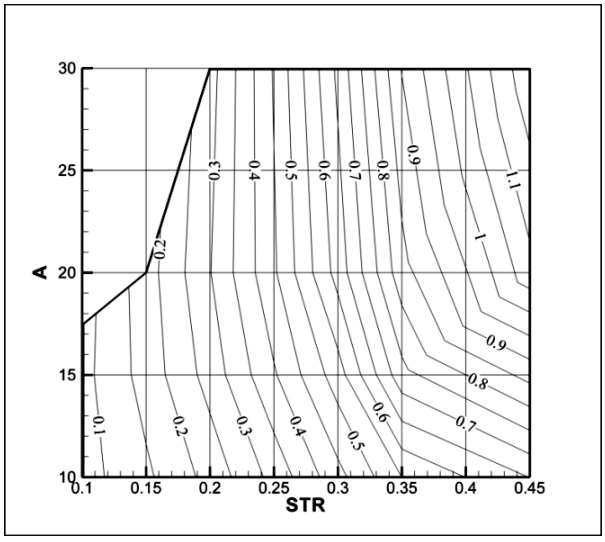

Fig. 2. Thrust coef., AR=6, rectangular wing.

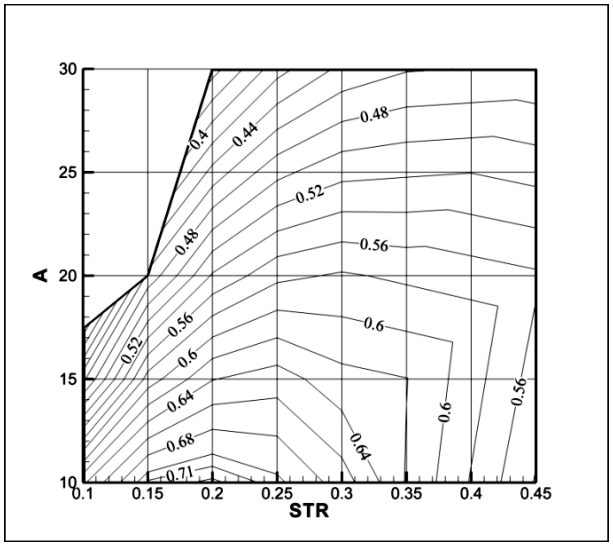

Fig. 3. Efficiency, AR=6, rectangular wing.

4.2 Rectangular wing, AR=3.

A rectangular wing with c=0.1 m and AR= 3 has been used in this calculation, fig. 4. All motion data is the same as previously. Calculation steps for $a_{\max}$ are 2.5 deg for this case.

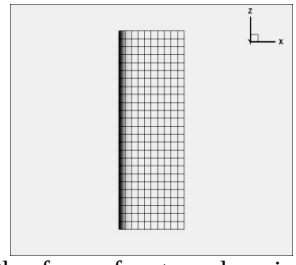

Fig. 4. Plan form of rectangular wing, AR=3

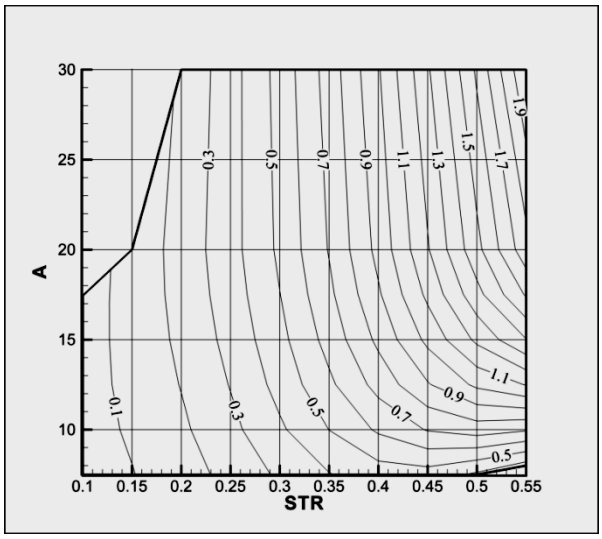

Fig. 5. Thrust coef., AR=3, rectangular wing.

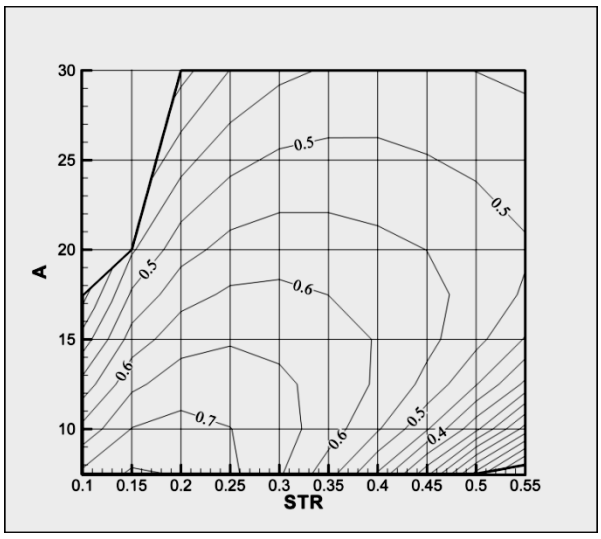

Fig. 6. Efficiency, AR=3, rectangular wing.

4.3 Two foil arrangement, AR=2.

Two rectangular wings operating in 180deg phase with c=1 m and AR= 2 have been used in this calculation, fig. 7. Motivation for this calculation has been taken from the work of Czarnowski J.T. (1997) at MIT. The wing distance (Y distance) has been selected to be 1.8m. Heave amplitude $y_0 = 0.75m$ and frequency $n = 3Hz$ have been used. The phase angle is $\psi = 90^0$ and a NACA0012 section has been used. Calculations have been performed with a step in St of 0.05 while steps in $a_{\max}$ are 5 deg.

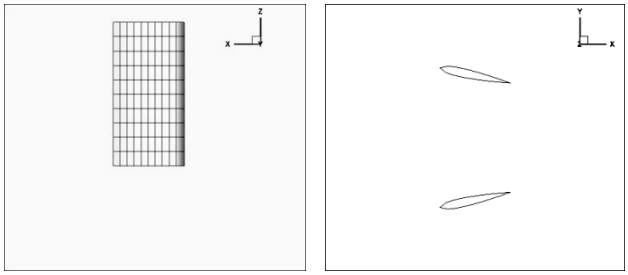

Fig. 7. Plan form of two foil arrangement, AR=2.

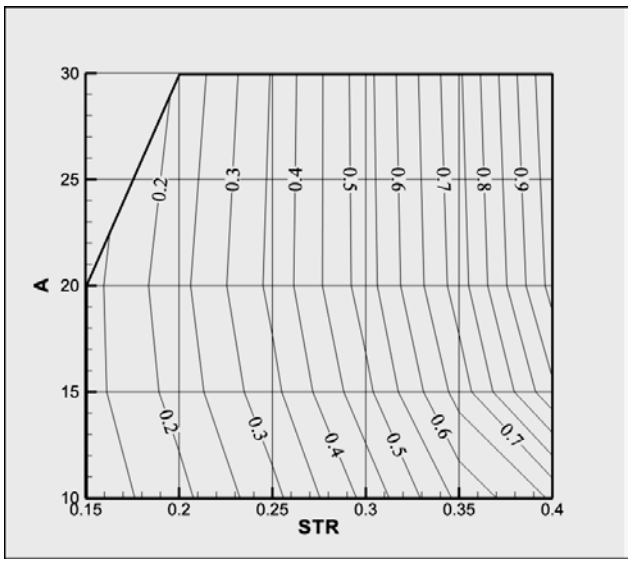

Fig. 8. Thrust coef., AR=2, two foil arrangement.

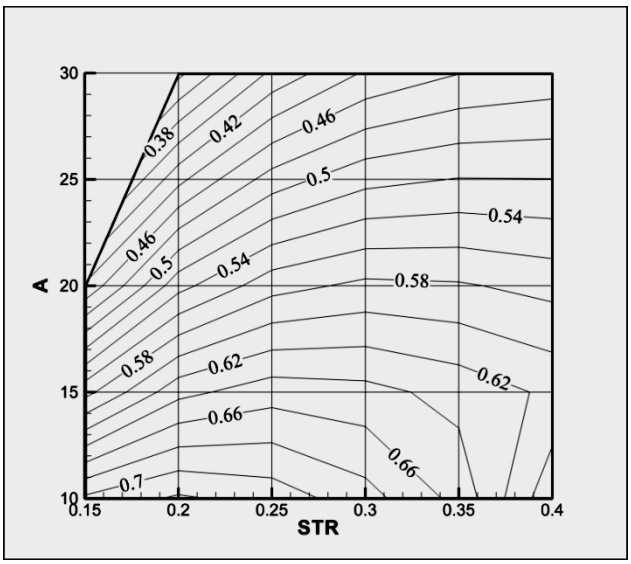

Fig. 9. Efficiency, AR=2, two foil arrangement.

4.4 Fish-like foil, AR=6, tapper=0.4, Skew-back=25 deg. The wing has mid-chord=1m, tip-chord=0.4m (tapper ratio=0.4), span s=6m, skew-back=25deg and a plan form which is fish-tail like, fig. 10. The plan form area of this wing is: $E = 4.64m^2$ leading to an AR= 7.76.

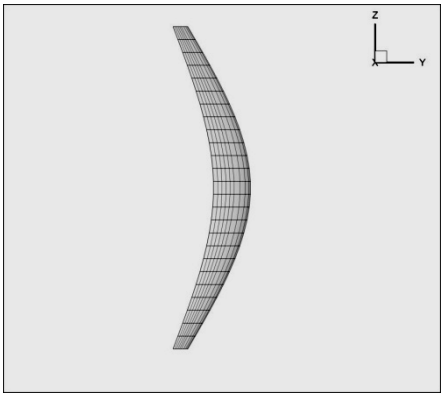

Fig. 10. Plan form of fish-tail like wing, skew-back=25deg, AR=7.76.

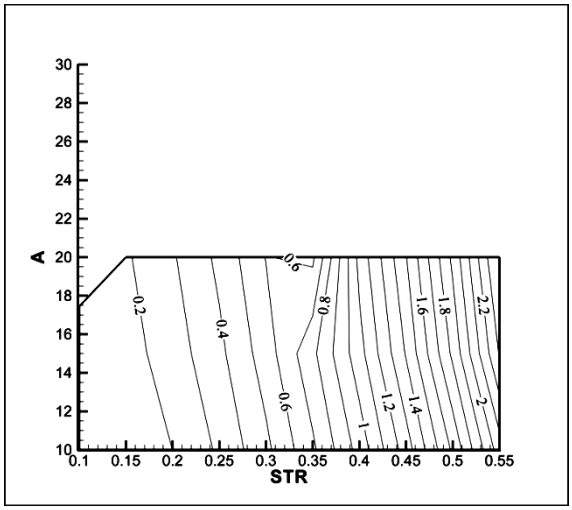

Fig. 11. Thrust coef. of fish-tail like wing, skew-back=25deg

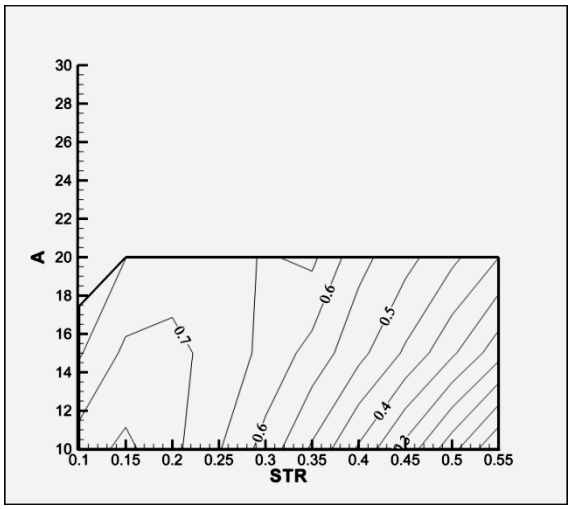

Fig. 12. Efficiency of fish-tail like wing, skew-back=25deg

4.5 Fish-like foil, AR=6, tapper=0.4, Skew-back=45 deg. The wing has mid-chord=1m, tip-chord= 0.4m (tapper ratio=0.4), span s=6m, skew-back=45deg and a plan form which is fish-tail like, fig. 13. The plan form area of this wing is: $E = 4.64m^2$ leading to an AR= 7.76.

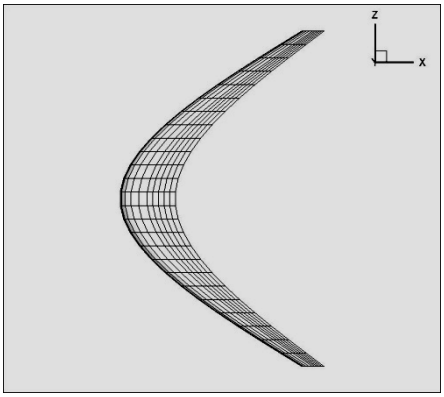

Fig. 13. Plan form of fish-tail like wing, skew-back=45deg, AR=7.76.

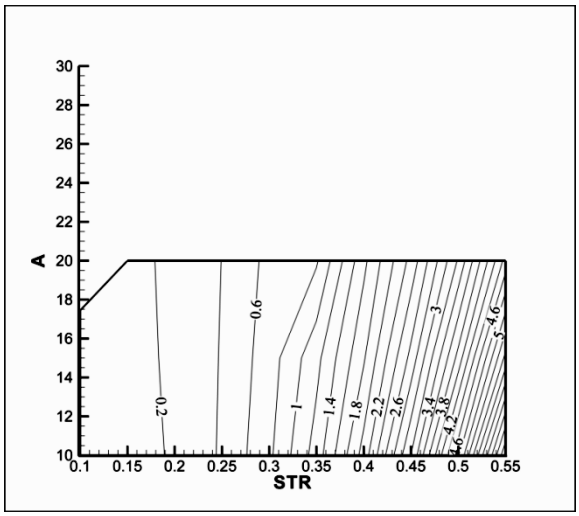

Fig. 14. Thrust coef. of fish-tail like wing, skew-back=45deg

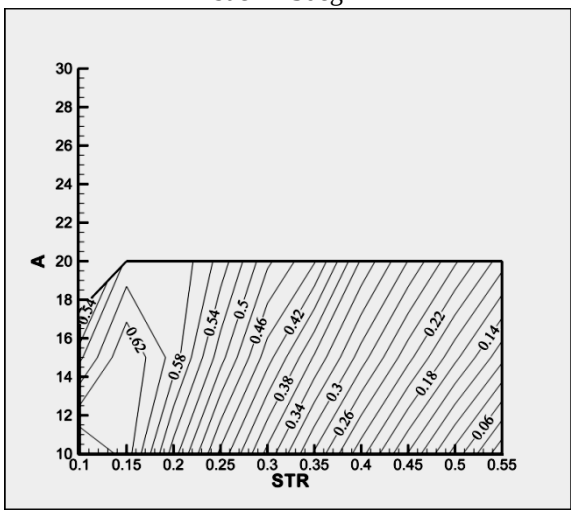

Fig. 15. Efficiency of fish-tail like wing, skew-back=45deg

4.6 An atlas of roll-up patterns.

We shall now present an atlas of some indicative vortex patterns observed in various flapping foil configurations with different loading conditions.

AR3 STR=0.15 A=7.5:

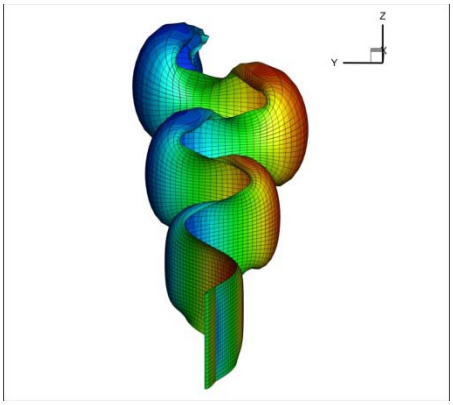

AR3 STR0.25 A=10

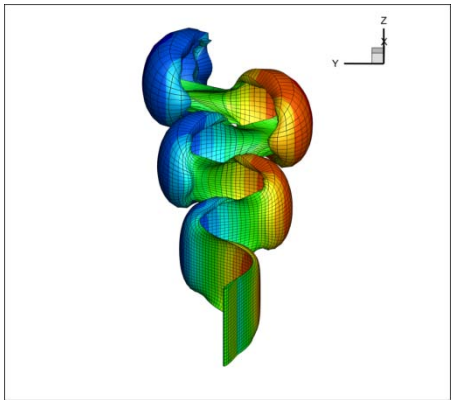

AR3 STR=0.35 A=17.5

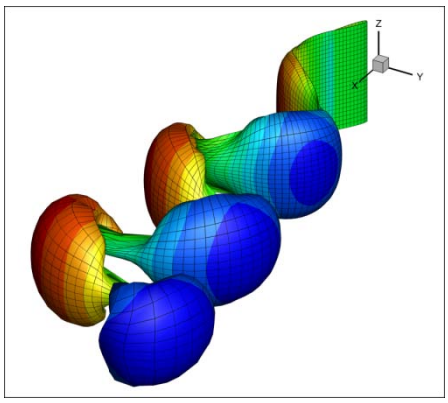

AR3 STR=0.45 A=20

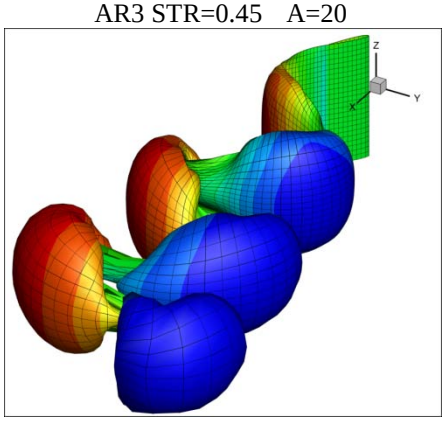

AR3 STR=0.55 A=30

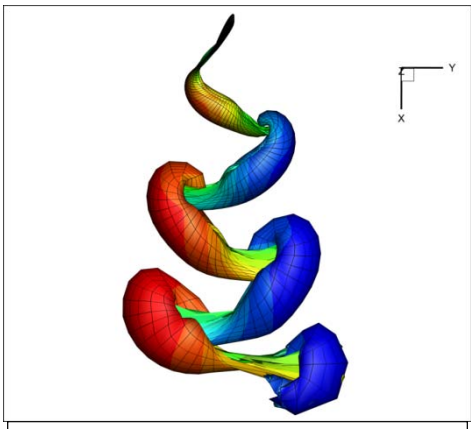

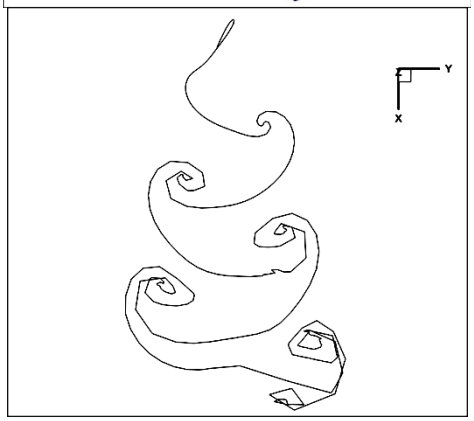

TWO RECTANGULAR FOILS AR=2 STR=0.4 A=15

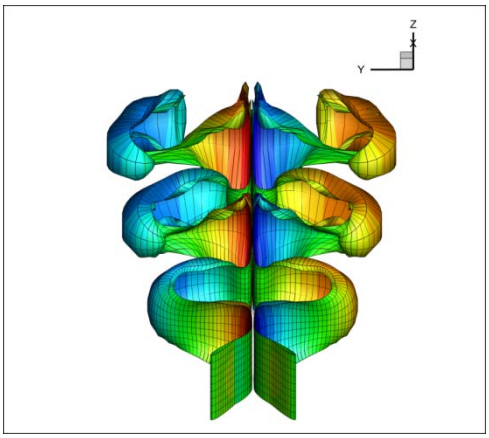

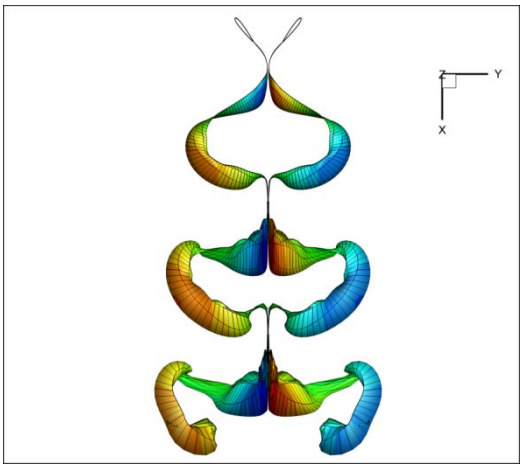

AR=7.76 SKEW=25 STR=0.45 A=20

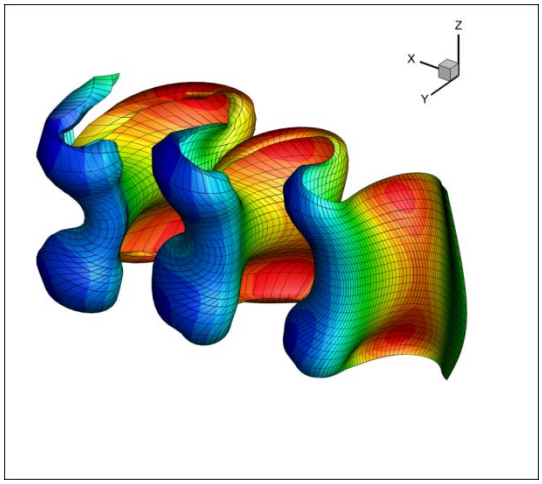

AR=7.76 SKEW=45 STR=0.45 A=20

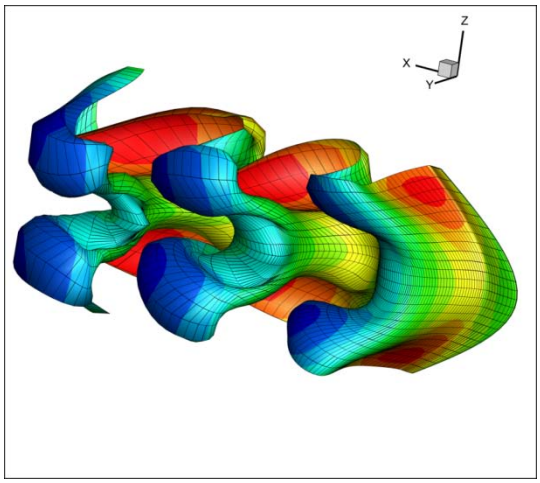

In the previous figures we verify the observations made by other researchers that the main mechanism of thrust production of flapping foils is the creation of an inverse Karman vortex street of ring shaped vortices. Of special interest are the vortex patterns of a fish tail-like wing where a double row of ring vortices is observed. Notice that those patterns are very similar to that obtained by a Navier Stokes solver, Borazjani and Sotiropoulos (2008).

5 COMPARISONS WITH EXPERIMENTS

In this section we present unsteady performance calculations for a rectangular wing with AR=6 and wing chord equal to 0.1 m. Professor Triantafyllou from MIT with his colleagues (Read, Hover, Triantafyllou, 2002) present experimental results for the aforementioned wing operating at various unsteady conditions. For the needs of the comparison we have selected an operating condition in which the wing produces both unsteady mean thrust and lift (named "pitch biased' condition). At the pitch biased condition the wing performs a parallel movement along X-axis with velocity u=0.4m/s, a heave motion given by:

$$y(t) = y_0 \sin(\omega t) \tag{11}$$

with $y_0 = 0.1m$ and $\omega = 5.0265 \cdot \mathrm{s}^{-1}$ and a pitching motion given by:

$$\theta(t) = \theta_0 \sin(\omega t + \psi) + \theta_{bias} \tag{12}$$

with $\theta_0 = 26.49\,\mathrm{deg}$, $\psi = 90\,\mathrm{deg}$ and $\theta_{bias} = 10\,\mathrm{deg}$.

The St number of the wing motion is equal to 0.4. With the selected parameters, the instantaneous angle of attack of the wing with respect to the instantaneous phenomenal velocity is given in figure 16. Notice that the instantaneous angle of attack for the selected condition ranges from -15 to 35 degrees.

Comparisons of the calculated time histories of thrust CT and lift CL coefficients with experimental results are shown on Figures 17 and 18. CT and CL are defined by (c: wing chord, s: wing span, ρ:density):

$$CT = \frac{T}{0.5\rho u^2 cs}, CL = \frac{L}{0.5\rho u^2 cs} \tag{13}$$

Very good coincidence of theoretical/numerical calculations with experimental results is observed. Notice that this coincidence was unexpected, since the instantaneous angles of incidence of the unsteadily moving wing reach the value of 35 deg (fig. 16) which is much greater than the static stall angle (between 10 and 15 deg). An explanation for this phenomenon is that unsteady motion of the wing acts as a boundary layer control mechanism which delays the bulk separation, to much higher angles of attack than that observed at a static condition.

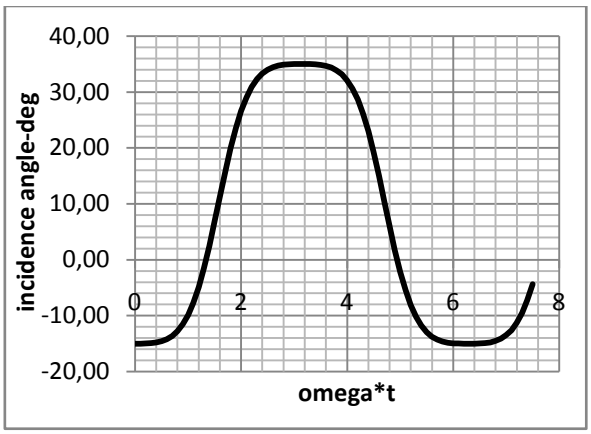

Fig. 16. Angle of attack vs time.

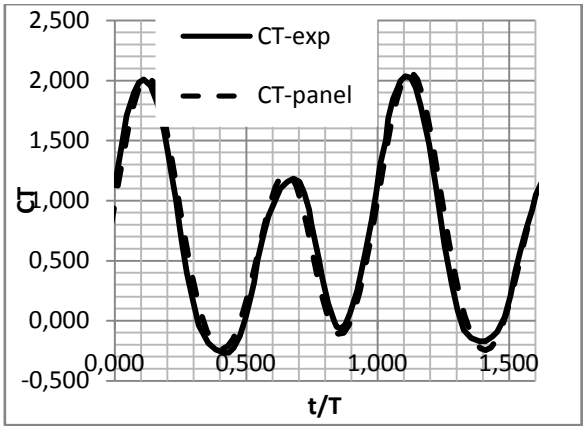

Fig. 17. Comparison of thrust coefficient.

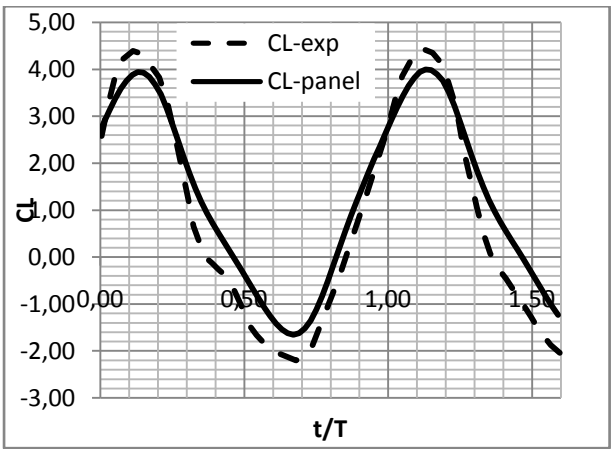

Fig. 18. Comparison of lift coefficient.

6 TWO FLEXIBLE FOILS IN FLAPPING AND TWISTING MOTION

As a final example we present unsteady performance calculations of a system of two flexible foils in flapping and twisting motion. The plan form of each airfoil in its neutral position is similar to that of section 4.1, fig.1. The tip sections of the foil are moving according to equations (8) or (9) and with the motion data given in section 4.1. A special data generation program deforms the foil using spline interpolation. During deformation, the plan form area of the foils is kept constant. This is a non-linear problem and thus a special Newton iteration is used at each time step to correct properly the area of the airfoil. Fig. 19 shows a view of the successive positions of the system of deformed airfoils.

Figure 20 shows the wake vortex pattern for this airfoil system. Notice that a double row of ring vortices is generated from each foil for this case. Figure 21 shows the powering and thrust performance of the foil system. Observe that this system produces a mean thrust force. Notice that in this figure we use the convention that positive power means useful power while negative power means consumed power. Thus EHP is almost always positive while DHP is almost always negative. In the same figure we have plot the Net-power (equation 5). Notice that there are time instances where net-power is positive i.e. our foil system absorbs energy from the flow.

7 CONCLUSIONS

A general boundary element code, for the treatment of unsteady incompressible non-viscous flows around systems of unsteadily moving rigid or flexible bodies, is presented. The code has systematically been applied for a number of foil configurations and design charts for such systems have been obtained. An atlas of wake vortex patterns for various foil plan forms and loading conditions is presented elucidating the thrust producing vortex mechanisms. The obtained design charts can be used for a preliminary design of flapping foil propulsion systems, while the final design and the fine-tuning and optimization of the system can be made afterwards using the developed BEM code. In the immediate future we plan to extend the presented data base to include more geometric and motion configurations as well as flexible wings.

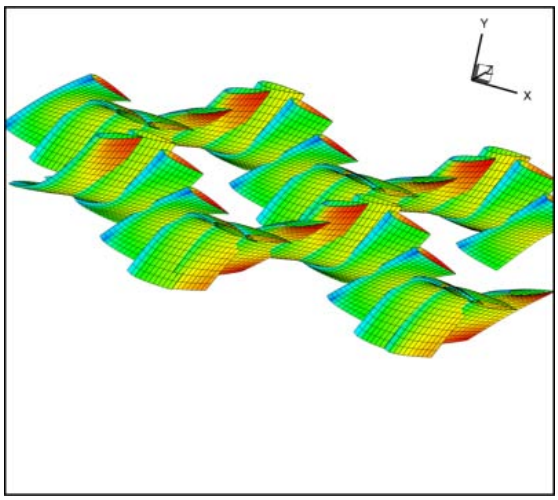

Fig. 19. View of successive positions of two flexible foils.

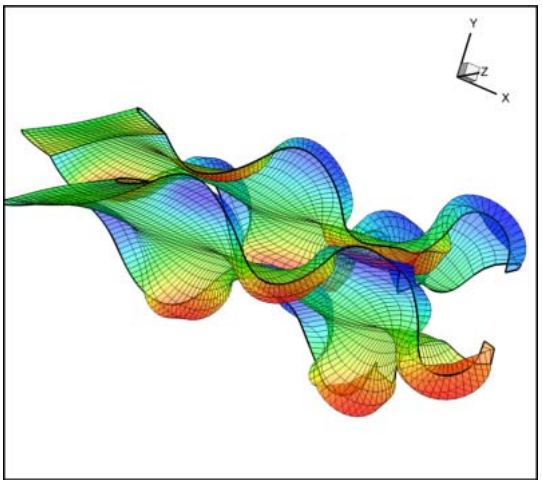

Fig. 20. Vortex pattern in the wake of two flexible foils.

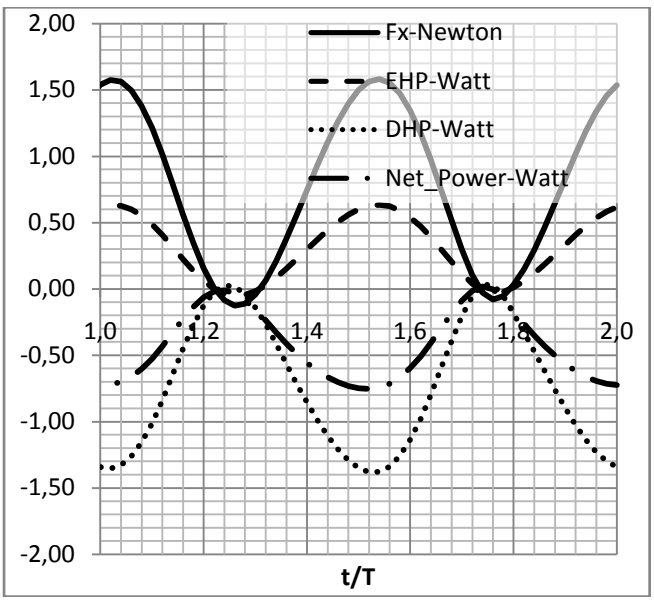

Fig. 21. Instantaneous values of axial force, EHP, DHP and Net-Power of two flexible foils.

REFERENCES

Anderson, J. M., Streitlien, K., Barrett, D. S. & Triantafyllou, M. S. (1998), 'Oscillating foils of high propulsive efficiency', J. Fluid Mech, vol. 360, pp.41-72.

Barrett D. S. , Triantafyllou M. S. (1999) 'Drag reduction in fish-like locomotion', J. Fluid Mech, vol. 392, pp.183-212.

Beal D.N. (2003) 'Propulsion through wake synchronization using a flapping foil', PhD thesis, MIT.

Borazjani I., Sotiropoulos F. (2008) 'Numerical investigation of the hydrodynamics of carangiform swimming in the transitional and inertial flow regimes', J. of Experimental Biology 211, 1541-1558.

Boss, N., (2008) 'Marine Powering Prediction and Propulsors', The Society of Naval Architects and Marine Engineers.

Czarnowski J.T. (1997) 'Exploring the possibility of placing traditional marine vessels under oscillating foil propulsion', MIT, Msc thesis.

Gopalkrishnan R., Triantafyllou M.S., Triantafyllou G.S., Barrett D. (1994) 'Active vorticity control in a shear flow using a flapping foil', J. Fluid Mech, vol. 274, pp.1-21.

Green M. A., Smits A. J. (2008) 'Effects of three-dimensionality on thrust production by a pitching panel', J. Fluid Mech, vol. 615, pp.211-220.

He M., Veitcha B., Bose N., Colbourne B., Liu P. (2006) 'A three-dimensional wake impingement model and applications on tandem oscillating foils', Ocean Engineering 34,1197-1210.

Hover, F. S., Haugsdal, O. & Triantafyllou, M. S. (2003) 'Control of angle of attack profiles in flapping foil propulsion', J. Fluids Struct.

Hover F.S., Haugsdal Ø., Triantafyllou M.S. (2004) 'Effect of angle of attack profiles in flapping foil propulsion', J. Fluids Struct. 19 (37-47)

Licht S., Hover F., Triantafyllou M.S. (2004) 'Design of a Flapping Foil Underwater Vehicle' IEEE J. of Oceanic Engineering, Vol.21, no 3.

Lighthill, M. J. (1969). Hydromechanics of aquatic propulsion: a survey. Annual Review of Fluid Mechanics 1, 413–446.

Liu P., Bose N. (1993) 'Propulsive performance of three naturally occurring oscillating propeller planforms'

Liu P., Bose N. (1997) 'Propulsive Performance from oscilating propulsors with spanwise flexibility', Proc. R. Soc. Lond. A 453,1763-1770.

Liu P., Bose N. (1999) 'Hydrodynamic characteristics of a lunate shape oscillating propulsor', Ocean Engineering 26, p.519-529.

Papaioannou G. (1997) 'Numerical simulation of unsteady separated flow around airfoils with applications to the propulsion of aquatic animals' Diploma Thesis, N.T.U.A.

Politis G.K., Belibasakis K.A., (1999) 'High propulsive efficiency by a system of oscillating wing tails', CMEM, WIT conference.

Politis G.K. (2004) 'Simulation of Unsteady motion of a Propeller in a fluid including Free Wake Modeling', Journal of Engineering Analysis with Boundary Elements, Vol 28, Issue 6, pp 633-653.

Politis G.K. (2005) 'Unsteady Rollup modeling for wake adapted propellers Using a time stepping method', Journal of Ship Research, Vol. 49, No 3.

Read D.A., Hover F.S., Triantafyllou M.S. July (2002) 'Forces on oscillating foils for propulsion and maneuvering', J. Fluids and Structures 17,163-183.

Sparenberg J. A. (2002) 'Survey of the mathematical theory of fish locomotion' ,J. Engineering Mathematics 44 (395-448).

Schouveiler L., Hover F.S., Triantafyllou M.S. (2005),'Performance of flapping foil propulsion', J. Fluids and Structures 20, 949-959.

Techet A. H., Triantafyllou M.S., Hover F. (2004) 'Review of Experimental Work in Biomimetic Foils' (IEEE)

Triantafyllou, M. S., Triantafyllou, G. S. & Gopalkrishnan R. (1991) 'Wake mechanics for thrust generation in oscillating foils', Phys. Fluids A 3(12).

Triantafyllou, M. S., Triantafyllou, G. S. & Grosenbaugh M.A. (1993) 'Optimal thrust development in oscillating foils with application to fish propulsion', Journal of Fluids and Structures 7, 205-224.

Triantafyllou, M. S., Triantafyllou, G. S. & Yue, D. K. P. (2000) 'Hydrodynamics of fishlike swimming' Annu. Rev. Fluid Mech.

Triantafyllou M. S., Techet A. H., Hover F. S. (2004) 'Review of Experimental Work in Biomimetic Foils', IEEE Journal of Oceanic Engineering, Vol. 29, No3.

Wu, T. Y. (1971). Hydromechanics of swimming propulsion. Part 1. Swimming of a two-dimensional flexible plate at variable forward speeds in an inviscid fluid. J. of Fluid Mechanics 46, 337–355.

Zhu Q., Wolfgang M.J., Yue D.K.P., Trianatafyllou M.S. (2002) 'Three dimensional flow structures and vorticity control in fish-like swimming', J. Fluid Mech., vol. 468, pp1-28.